

Implementation of a parameter identification method for transient modeling of EC motors using the software *opera*

Master Thesis

Ehsan Anaraki Mohammadi

Mat.-Nr.: 2906150

Date: 05.12.2012

**Institute for Drive Systems and Power Electronics
Leibniz Universität Hannover**

First examiner:

Prof. Dr.-Ing. Bernd Ponick

Second examiner:

Prof. Dr.-Ing. Axel Mertens

Supervisor:

Dr-Ing. Cornelia Stübig

I hereby declare that I have written this thesis myself, and that I have not used any other sources or tools than the ones mentioned in this work.

Hannover,,.....

Contents

CONTENTS	I
SYMBOLS	II
ABBREVIATION	II
LIST OF FIGURES	III
ABSTRACT	5
1 INTRODUCTION	6
1.1 MOTIVATION AND OBJECTIVES	6
2 BASICS	8
2.1 BLDC FUNDAMENTALS	9
2.1.1 Stator.....	9
2.1.2 Rotor.....	11
2.1.3 Electronic parts.....	12
2.1.4 Motor characteristic.....	13
2.1.5 Theory of application.....	15
2.2 PARK TRANSFORMATION.....	16
2.3 BLDC EQUIVALENT CIRCUIT	19
2.3.1 Mathematical Model.....	19
2.3.2 Transient model.....	22
2.4 DETERMINATION OF THE MACHINE PARAMETERS USING SOFTWARE OPERA	25
2.4.1 Stator parameters.....	25
2.4.2 Rotor parameters.....	26
3 SIMULATION USING THE SOFTWARE OPERA	29
3.1 INTRODUCTION.....	29
3.2 MODEL CREATION.....	29
3.2.1 Rotor.....	29
3.2.2 Stator.....	30
3.2.2.1 Default stator geometry	30
3.2.2.2 Integrated stator	30
3.2.3 Functional region.....	31
3.3 CODING IN SOFTWARE OPERA	37
4 RESULT	43
4.1 STATOR INDUCTANCES IDENTIFICATION	43
4.2 ROTOR PARAMETERS IDENTIFICATION	52
5 CONCLUSION	58
REFERENCES:	59
APPENDIX	61

Symbols

A	Vector potential
B	Magnetic flux density
\underline{d}	Field dampening factor
f	Frequency
H	Magnetic field strength
i	Current
J	Current density
L	Self inductance
L_h	Magnetising inductance
L_σ	Leakage inductance
n	Speed
p	Pole pairs
u	Voltage
R	Resistance
S	Slip
θ	Angle of phase shift
v	Order number
ψ	Flux linkage
ω	angular velocity

Abbreviation

BLDC	Brushless direct current
DC	Direct current
EC	Electrically commutated
IPM	Interior mounted permanent magnet
SPM	Surface mounted permanent magnet
AC	Alternative current
RM	Rotating machine

List of Figures

Figures:

Figure 2.1: A BLDC schema [1].....	8
Figure 2.2: Winding distributions for the 12-slot/10-pole motors. (a) All teeth wound. (b) Alternate teeth wound. (c) Alternate teeth wound on wider teeth.[5].....	10
Figure 2.3: Cross-section of a 4-pole brushless motor (left) surface mounted permanent magnets (right) interior PM motor. Magnets of North and South polarity are shown in red and blue [7]......	11
Figure 2.4: (a) Practical circuit for a three-phase bipolar-driven motor (b) arrangement of Hall elements [8]	12
Figure 2.5: Hall sensor output, Back-EMF, Output torque and current of a typical BLDC [3]	14
Figure 2.6: The windings energizing modes during six-step commutation sequences[3]	15
Figure 2.7: Clarke's current vectors in abc system [10].....	17
Figure 2.8: Park's current vectors in Clarke's system [10]	18
Figure 2.9: The equivalent circuit of a BLDC motor in dq system [11].....	21
Figure 2.10: Equivalent circuit for BLDC in d and q -axis with respect to eddy currents[12].....	23
Figure 3.1: (a) Interior mounted permanent magnet rotor IPM.....	30
Figure 3.2: Opera Scripts for creating integrated stator.....	31
Figure 3.3: Current Density figure (a) 3d,(b)2d.....	32
Figure 3.4: Flux Lines created by functional layer when factor a equals 5 before changing the functional region	33
Figure 3.5: Flux Lines created by dividing layer.....	34
Figure 3.6: The flux that is created by the sinusoidal current density with order 15	36
Figure 3.7: Opera scripts for creating functional regions	37
Figure 3.8: Codes for applying orders and frequencies setting	38
Figure 3.9: Codes for generating a loop for changing number of poles in each step	39
Figure 3.10: Codes for solving and generating a loop to change frequency in each step	41
Figure 3.11: Codes for generating data table.....	42
Figure 4.1: IPM and axis directions (a) d -axis (b) q -axis	43
Figure 4.2: SPM and axis directions (a) d -axis (b) q -axis	44
Figure 4.3:Flux density and Fourier series of flux density in air-gap for SPM rotor in d axis.....	45
Figure 4.4: Flux density and Fourier series of flux density in air-gap for SPM rotor in q axis.....	45
Figure 4.5: Flux density and Fourier series of flux density in air-gap for IPM rotor in d axis.....	46
Figure 4.6: Flux density and Fourier series of flux density in air-gap for IPM rotor in q axis.....	47
Figure 4.7: The functional region (red region) that creates the sinusoidal flux density. 53	
Figure 4.8 : d and q position of the rotor in $v = p = 5$ harmonic	54
Figure 4.9: d and q position of the rotor in $v = 19$ harmonic	54

Diagrams:

Diagram 3.1: Generated current density in region when $a=5$ before changing the functional region	33
Diagram 3.2: Generated poles after dividing	34
Diagram 3.3: Current density in the functional region for creating 15 th order flux density	35
Diagram 3.4: Vector potential in the functional region created by 15 th order current density	35
Diagram 4.1: Values of different harmonic orders for SPM rotor	46
Diagram 4.2: Values of different harmonic orders for IPM rotor	47
Diagram 4.3: variations of flux density in the different rotor angles	48
Diagram 4.4: Percentage of magnitude of spatial harmonics with respect to rotor angle for different orders for IPM rotor	48
Diagram 4.5: Percentage of magnitude of spatial harmonics with respect to rotor angle for different orders for SPM rotor	49
Diagram 4.6: Flux density of IPM and SPM rotor in α axis direction	50
Diagram 4.7: Flux density of IPM and SPM rotor in β axis direction	50
Diagram 4.8: Absolute value of the field-dampening factor for $p = v = 5$	55
Diagram 4.9: Variations of Dampening factor with respect to frequency for the order ($v = p$)	55
Diagram 4.10: Resistances of the fictive damper winding for 5 th order	56
Diagram 4.11: Inductances of the fictive damper winding for 5 th order	56

Tables:

Table 4.1: Inductances for SPM rotor	51
Table 4.2: Inductances for IPM rotor	52
Table 4.3: Averaged Reluctances of the fictive damper windings	57
Table 4.4: Averaged leakage inductances of the fictive damper windings	57

Abstract

Topic of this thesis:

Implementation of a parameter identification method for transient modeling of EC motors using the software *opera*

The Finite Element software *opera* is used by a motor manufacturer to calculate the stationary behavior of EC motors. Several scripts are already implemented for this task. Transient behavior, however, is efficiently analyzed by analytical approaches better than by FEM. Nevertheless, the motor parameters required for the analytical model must be identified via FEM.

In this thesis, a parameter identification method for EC motors shall be implemented. In this method, the rotor is excited by an alternating harmonic field, and its harmonic response is determined. To achieve this goal, an existing script file for calculation of EC motors in *opera* has to be adapted to calculate the rotor's equivalent circuit parameters.

1 Introduction

1.1 Motivation and objectives

Brushless direct current motors or BLDC motors are part of the electrically commutated (EC) motors. According to its name, this motor works with DC power however there is not any direct electrical connection contact between electrical parts of the stator and the rotor. This leads to having advantages of both DC and induction motors together. Some of them are listed below:

- 1) Ease of speed control
- 2) High dynamic response
- 3) Working at high-speed uses
- 4) Noiseless operation
- 5) Long life
- 6) High efficiency (because of lower losses)
- 7) Notable torque to size ratio

Technological progress made the BLDC motor production process easier and cheaper. Above reasons increase using of BLDC motors in industries rapidly [2], [3].

This increasing tendency to use of BLDC motors induces the requirement of accurate electrical equivalent model for exact behavior analysis. Eddy currents will occur in the conducting regions of the rotor. These effects happening in steady-state condition due to spatial harmonic fields of the winding are neglected in most conventional models, even though in some occasion like stators consist of tooth-wound coils cause a generally undesired and different spatial harmonics that increases rotor losses and has to be considered.[4]

An enhanced model involving the eddy current losses is used to identify the parameters of motor, which is presented in the next chapter.

2 Basics

BLDC motors can be categorized as synchronous motors. This means that there is no slip like the one exists in induction motors here, and the rotor rotates at the speed of the rotating magnetic field generated by the stator winding.



Figure 2.1: A BLDC schema [1]

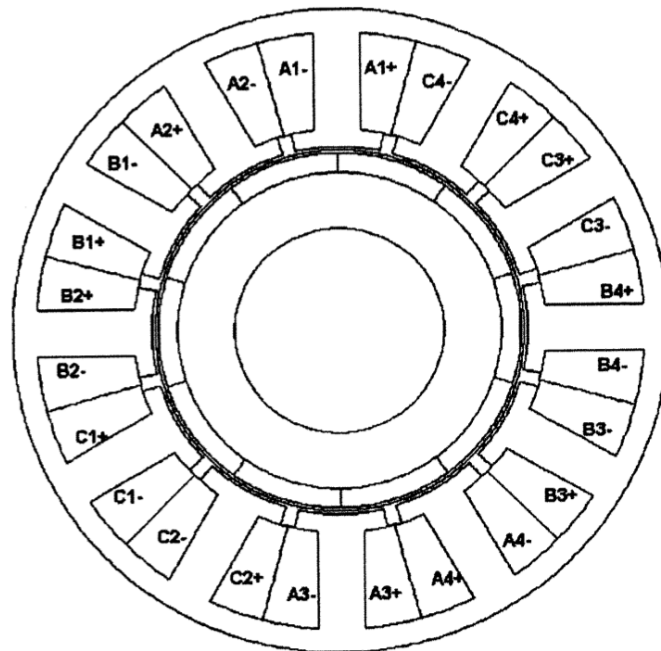
2.1 BLDC fundamentals

A BLDC motor consists of three main sections:

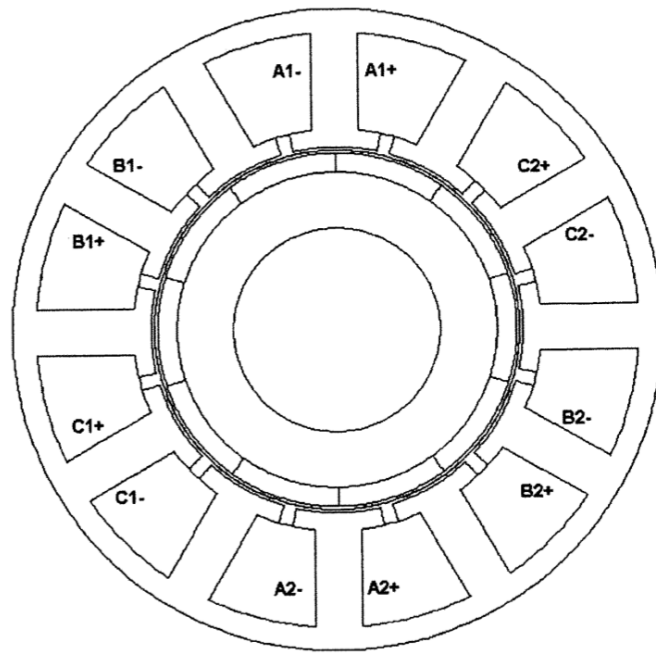
- I. Stator
- II. Rotor
- III. Electronic part including hall sensors

2.1.1 Stator

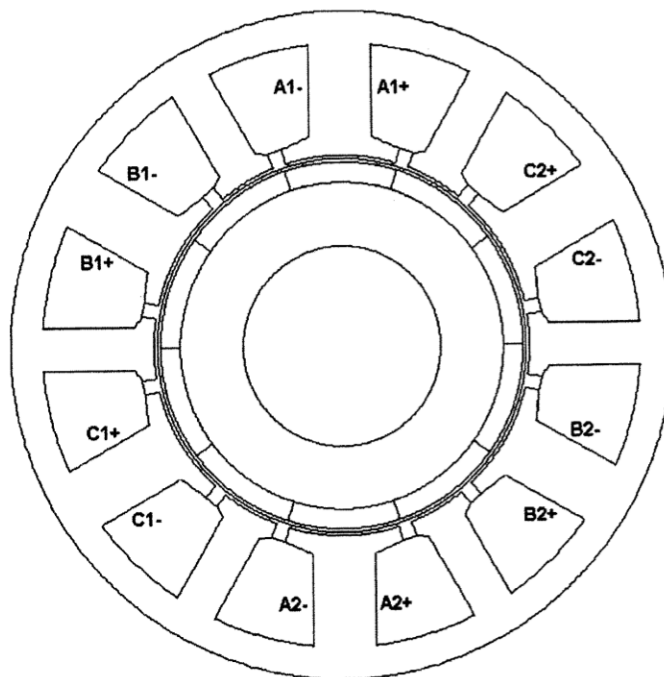
Most conventional BLDC motors have three phases winding in the stator, but this is not always the case. According to required performance, the phase numbers can be increased or decreased. The stator of a BLDC motor basically is the same as that is used in the induction motors, but due to technical requirements the windings are distributed in different ways in the slots. Some different kinds of winding schemes are illustrated in Figure 2.2.



(a)



(b)



(c)

Figure 2.2: Winding distributions for the 12-slot/10-pole motors. (a) All teeth wound. (b) Alternate teeth wound. (c) Alternate teeth wound on wider teeth.[5]

Stator is formed normally from stacked steel laminations [5]. It is important to have a uniform torque during motor application and this is achieved by matching the armature

linkage fluxes, the current waveforms and the winding design [2]. The number of stator slots is chosen depending on the rotor poles, phase number, and the winding configuration. In general, a fractional slots/pole design is preferred to minimize cogging torque [6].

2.1.2 Rotor

Main distinction between EC motors and the other types of motors is using of permanent magnet in their rotor. Brushless permanent magnet (BLPM) motors can be classified in two major groups: motors with the PM mounted on the surface of the rotor which is known as SPM and the second category is motors with PM placed in the interior of the rotor body which is called IPM. The production procedure of first group is gluing arc magnets and securing them with special tape on the outer surface of a rotor core. This is cost effective when large ferrite magnets or bonded magnet rings are used, however, it presents challenges for the sintered NdFeB designs.

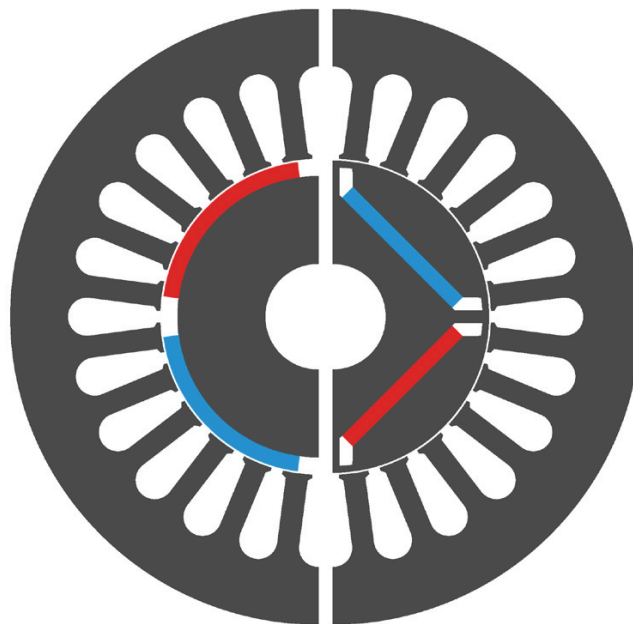


Figure 2.3: Cross-section of a 4-pole brushless motor (left) surface mounted permanent magnets (right) interior PM motor. Magnets of North and South polarity are shown in red and blue [7].

On the other hand due to rectangular shape of permanent magnets that is used in IPMs the manufacturing process will be simplified and cost effective. There are a large variety of designs for EC rotors; shown in Figure 2.3 are the most common types [7].

2.1.3 Electronic parts

As in these motors commutation is controlled electronically, they are named as Electronically Commutated (EC) motors. The position of rotor has to be identified indirectly because there is no direct electrical connection between rotating part and armature as in conventional DC motors. Mechanical contact is not used in the BLDC because it will reduce the efficiency and longevity.

Different sensors can be applied to detect the exact rotor position in BLDC motor. Also some sensor-less methods are employed to control this motor.

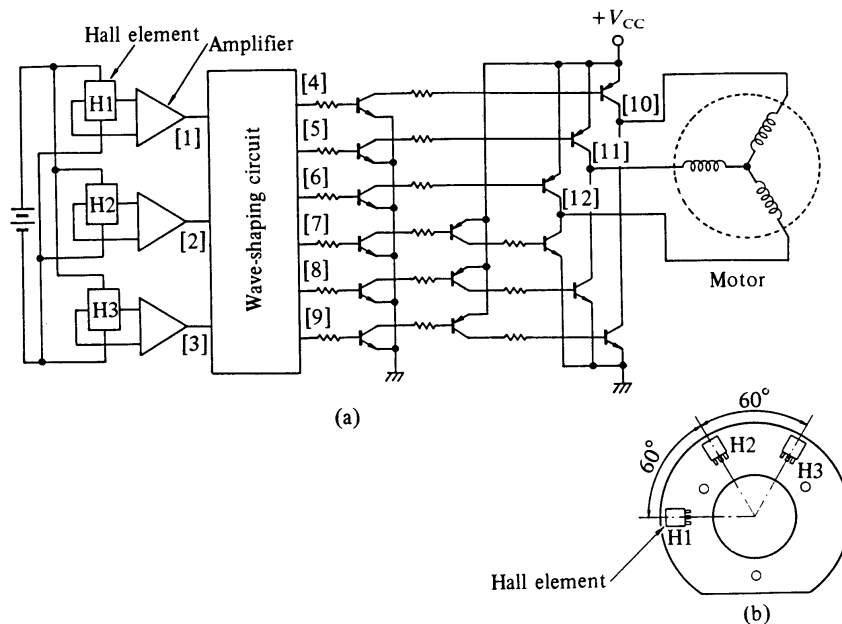


Figure 2.4: (a) Practical circuit for a three-phase bipolar-driven motor (b) arrangement of Hall elements [8]

Figure 1.2 illustrates the circuit of a typical three-phase brushless DC motor with the position of hall sensors, which are used for identifying rotor angle.

2.1.4 Motor characteristic

The air-gap flux-density waveform of BLDC is essentially a square wave, but fringing causes the corners to be somewhat rounded. As the rotor rotates, the waveform of the voltage induced in each phase with respect to time is an exact replica of the air-gap flux-density waveform with respect to rotor position. The fringing leads to a trapezoidal style to EMF that discriminate between BLDC and PMSM motor that have a sinusoidal EMF. In a three phase BLDC the EMF that induced in each phase are the same in the shape but have 120° electrical shift in phase angle. By exciting the stator phases by a rectangular current in the correct time an almost constant torque is achievable. [6].

The amplitude of the phase back-EMF is relative to the rotor speed, and is given by:

$$U = k\phi\omega_m \quad (2.1)$$

That ω_m is mechanical speed, ϕ is the permanent magnet flux and k is a constant factor that is relative to phase turns.

The instantaneous power in every 120° interval, is the sum of the contributions from two phases in series, which can be formulated by:

$$P_o = \omega_m T_e = 2UI \quad (2.2)$$

Where T_e is the output torque and I is the amplitude of the phase current. The equation for the output torque can be extracted from equation (2.1) and (2.2)

$$T_e = 2k\phi I = k_t I \quad (2.3)$$

Where k_t is the torque constant. From equation (2.1) and (2.3) the resemblance between BLDC motor and conventional DC motors (brushed) can be observed easily [6].

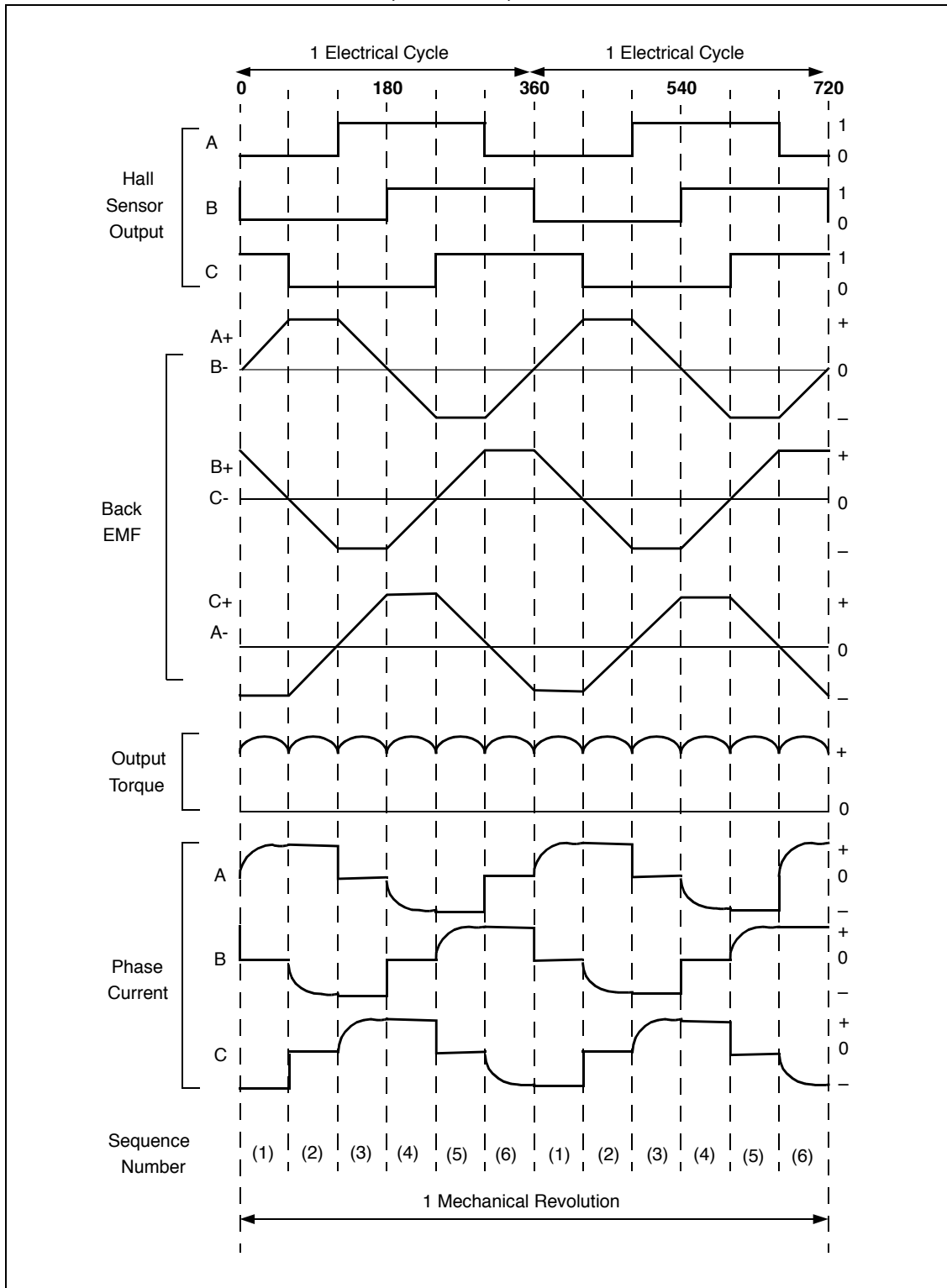


Figure 2.5: Hall sensor output, Back-EMF, Output torque and current of a typical BLDC [3]

2.1.5 Theory of application

In each commutation sequence, one of the stator windings is excited with positive power (current enters into winding), the second one has negative power and the third one has no power. The generated magnetic field interacts with the rotor permanent magnets, and rotor starts rotating. Shifting in position of stator magnetic field keeps motor rotating, and this is the reason that energizing sequence of stator windings is dependent upon the rotor position. What is known as “Six-step Commutation”, is a method that defines sequences of energizing.

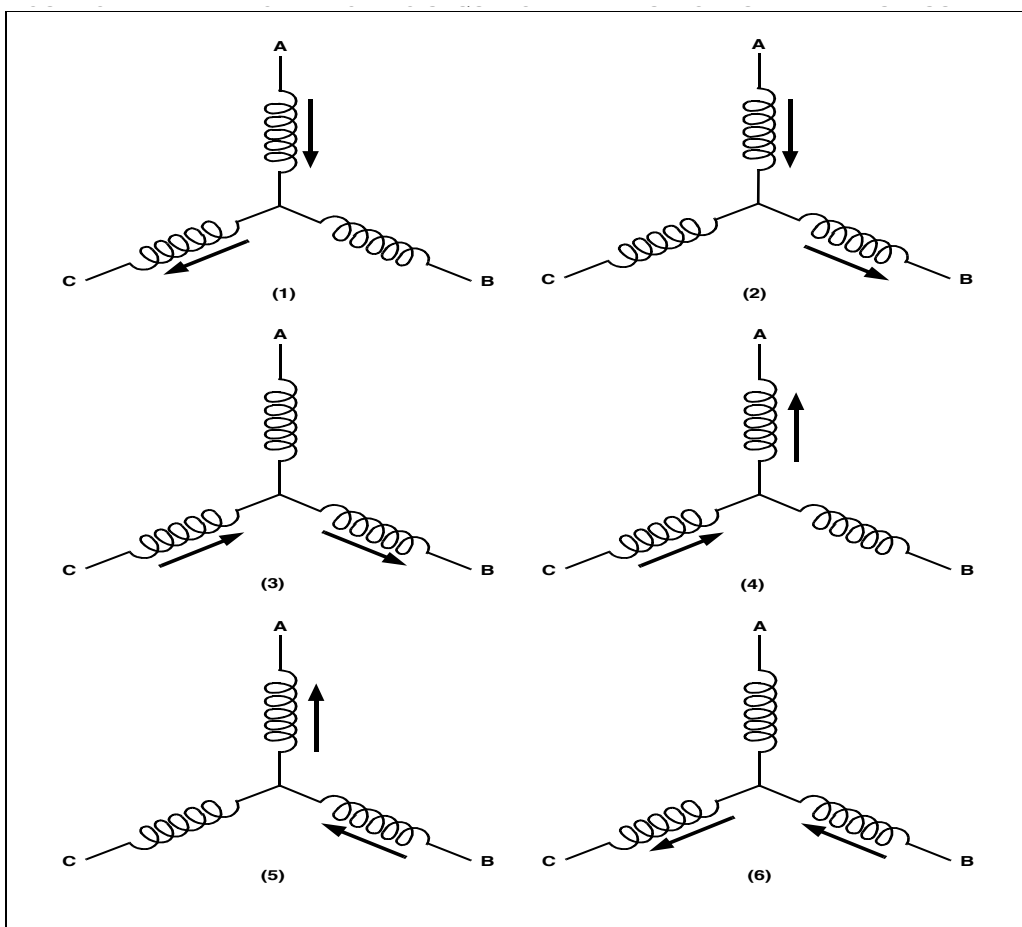


Figure 2.6: The windings energizing modes during six-step commutation sequences[3]

In this method the controller in BLDC finds sequence number with respect to the predicted or sensed rotor position, and switches DC power between the stator windings, according to the template that is depicted in the Figure 2.6 [6].

2.2 Park transformation

The direction and magnitude of the magnetic field is equal to the sum of the current vectors of different phases. Thus by measuring the currents through each phase the total current vector can be calculated

A ‘Clarke transformation’ is used to convert a 3-phase system into a 2-phase coordinate system. This frame is called static reference frame. The quadrature-phase components can be calculated using only two phases of the 3-phase system.

$$I_{\alpha\beta\gamma} = T I_{abc} = \begin{bmatrix} 1 & -\frac{1}{2} & -\frac{1}{2} \\ 0 & \frac{\sqrt{3}}{2} & -\frac{\sqrt{3}}{2} \\ \frac{1}{2} & \frac{1}{2} & \frac{1}{2} \end{bmatrix} \begin{bmatrix} I_a \\ I_b \\ I_c \end{bmatrix} \quad (2.4)$$

Alternatively, the scaling of the transformation can be chosen to $\sqrt{2/3}$ instead of $2/3$ in a balanced system $I_a + I_b + I_c = 0$, and thus $I_\gamma = 0$ and two of the phase currents suffice to calculate the α and β components. In this case the transform simplifies to

$$I_{\alpha\beta} = \begin{bmatrix} 1 & 0 \\ \frac{1}{\sqrt{3}} & \frac{2}{\sqrt{3}} \end{bmatrix} \begin{bmatrix} I_a \\ I_b \end{bmatrix} \quad (2.5)$$

Based on [9], This leads to a non power-invariant transformation:

$$I_\alpha = I_a \quad (2.6)$$

$$I_\beta = \frac{(I_a + 2I_b)}{\sqrt{3}} \quad (2.7)$$

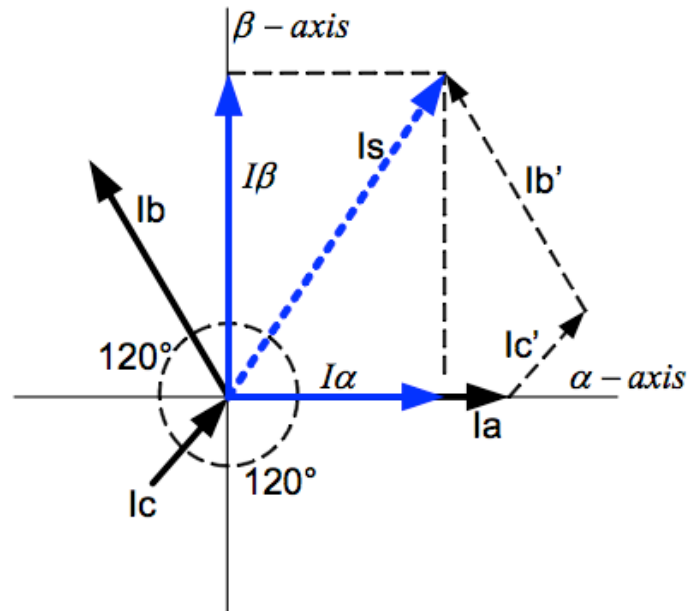


Figure 2.7: Clarke's current vectors in abc system [10]

The current vector in the static reference frame (α , β) of the windings can be transformed into the dynamic frame (d , q) of the rotating permanent magnet to create a speed invariant system

A Park transformation is used to transform the static reference frame to a dynamic reference frame. In a zero speed situation

$$I_d = I_\beta \sin \alpha + I_\alpha \cos \alpha \quad (2.8)$$

$$I_q = I_\beta \cos \alpha - I_\alpha \sin \alpha \quad (2.9)$$

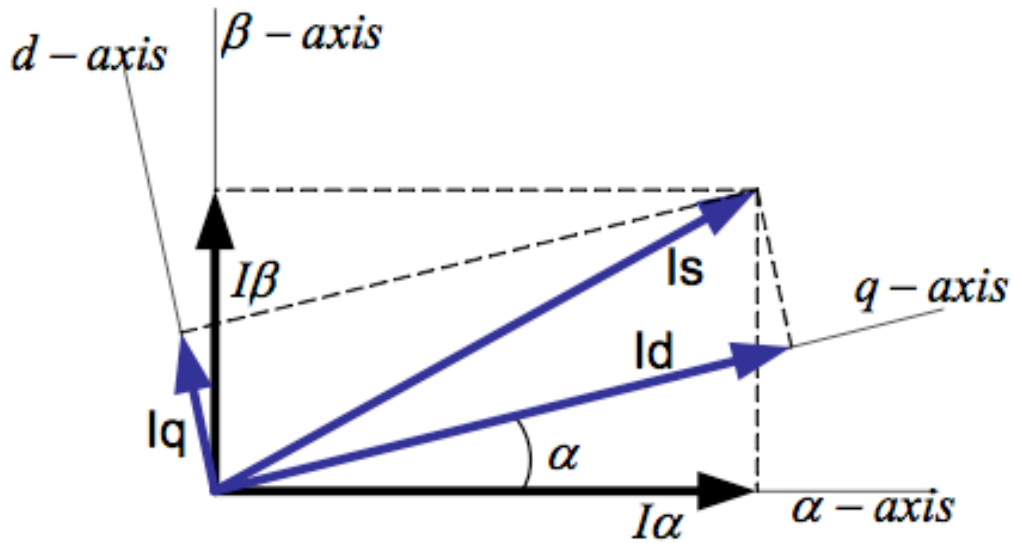


Figure 2.8: Park's current vectors in Clarke's system [10]

According to eq. (2.8) and (2.9), in order to find I_d and I_q the first step is calculating I_α, I_β and α . I_α and I_β can be calculated based on eq.(2.6) and (2.7). But α is still unknown. Assume that the aim is finding I_d when rotor is oriented on d -axis. Therefore it is necessary to know direction of d -axis. When rotor is oriented on d , I_q is zero. This means:

$$\alpha = \text{tg}^{-1} \frac{I_\beta}{I_\alpha} \quad (2.10)$$

By substituting eq. (2.8) and (2.9) into eq. (2.10):

$$\alpha = \text{tg}^{-1} \frac{I_a + 2I_b}{\sqrt{3}I_a} \quad (2.11)$$

Finally according to eq. (2.6) to (2.9) and (2.11):